Chinese Chemical Letters 31 (2020) 2023–2026

Contents lists available at ScienceDirect

Chinese Chemical Letters

journal homepage: www.elsevier.com/locate/cclet

Communication

Control of random self-assembly of pyrogallol[4]arene-based nanocapsule or framework

Kongzhao Su[a,b], Shunfu Du[a,c], Wenjing Wang[a,b], Daqiang Yuan[a,b,*]

[a] State Key Laboratory of Structural Chemistry, Fujian Institute of Research on the Structure of Matter, Chinese Academy of Sciences, Fuzhou 350002, China
[b] University of the Chinese Academy of Sciences, Beijing 100049, China
[c] College of Chemistry, Fuzhou University, Fuzhou 350116, China

ARTICLE INFO

Article history:
Received 25 October 2019
Received in revised form 26 November 2019
Accepted 28 November 2019
Available online 29 November 2019

Keywords:
Controlled assembly
Pyrogallol[4]arene
Metal-organic nanocapsule
Metal-organic framework
Magnetism

ABSTRACT

The controlled self-assembly of discrete metal-organic nanocapsules (MONCs), and metal-organic frameworks (MOFs) based on the MONCs are achieved. Specifically, the solvothermal reaction of nickel nitrate hexahydrate and *C*-methylpyrogallol[4]arene in mixed DMF/MeOH solution leads to the unexpected form of discrete nickel-seamed hexameric pyrogallol[4]arene MONCs, and MONC-based three-dimensional (3D) MOF. Notably, the latter MOF is constructed from the aforementioned nickel-seamed MONC building blocks and formate linkers *in-situ* generated from the hydrolysis of DMF solvent. Interestingly, introducing pyridine and formic acid in the reaction conditions leads to the controlled assemblies of the discrete MONC and MONC-based 3D MOF structures. Moreover, the variable-temperature magnetic susceptibilities of both the abovementioned compounds have been investigated, indicating typical antiferromagnetic interactions between the metal centers.

Research into controlled self-assembly of molecular species into well-defined hierarchical architectures has attracted much interest recently, because it has not only been determined to be extremely valuable in the preparation of functional materials, but also important to understand the self-assembly processes in nature [1–3]. In the past few decades, chemists have prepared a variety of hierarchical metal-organic frameworks (MOFs) from metal ions/clusters and organic linkers [4–11]. However, utilization of the nanometric building blocks (NBBs), which are comparable complexity to biological species, in preparation of MOFs still remains a significant challenge [12–15].

Supramolecular nanocapsules with inherent large cavities have attracted much interest due to their potential applications in many areas including gas adsorption/separation, catalysis, molecular encapsulation [16–19]. Up to now, the number of known MOFs made from supramolecular nanocapsules is still limited. For instance, Cooper *et al.* firstly reported a three-dimensional (3D) cage-MOF composed of a dodecaamine organic cage as linker and Zn_6 cluster as node in 2010 [12]. Ma and co-workers succeed in controlling assembly of two-dimensional (2D) or 3D framework structures by using isolated rhombihexahedron Cu_{24} coordination nanocages as NBBs *via* a coordination-driven polymerization method in 2015 [13]. Pan *et al.* prepared a sodium-directed networked cage from a triangular prism-shaped porous organic cage in 2017 [14]. Very recently, Kim and co-workers presented a rational approach to the design and construction MOFs constructed from corner-truncated cubic zinc-metallated porphyrin boxes as NBBs and ditopic bridging ligands. Despite the success, the design and construction of nanocapsule-based MOFs are still in the embryonic stage of development, lots of efforts still need to be done to obtain such kind of MOFs [15].

Pyrogallol[4]arenes (PgC_ns, where n is the number of carbon atoms in pendant alkyl chains), bowl-shaped molecules with four pyrogallol (Pg) groups, can coordinate to a variety of metal ions such as Mg, V, Mn, Fe, Co, Ni, Cu, Zn, Ga and Ln (lanthanide) to form dimeric and/or hexameric metal-organic nanocapsules (MONCs) [20–24]. Interestingly, such dimeric and hexameric MONCs can be used as NBBs to build hierarchical architectures. For example, the dimeric Cu- and Zn-seamed MONCs can be linked into one-dimensional (1D) chain and 2D network with 4,4′-bipyridine ligand [25,26], respectively, while the larger hexameric Mg- and Ni-seamed MONCs can self-organize into various 2D and 3D MOFs by connecting the tailed hydroxyl groups of the bifunctional PgC_3OH ligands with adjacent hexameric nanocapsules via metal-hydroxyl coordination [27,28].

* Corresponding author.
E-mail address: ydq@fjirsm.ac.cn (D. Yuan).

https://doi.org/10.1016/j.cclet.2019.11.047
1001-8417/

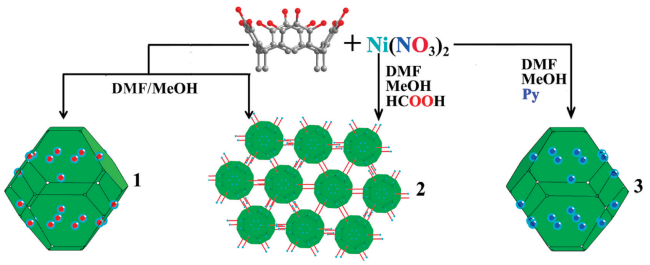

Scheme 1. Random to the controlled assembly of discrete nickel-seamed MONC and MONC-based MOF. Red and blue circles stand for metal coordinate to oxygen and nitrogen, respectively.

Formate, the simplest carboxylate, has been determined to be an excellent organic linker with a variety of coordination modes owing to the smallest possible side group on the carboxylate carbon. More interestingly, it can be generated in situ from the hydrolysis of amide-based solvents under solvothermal conditions [24]. Up to now, a lot of fascinating metal-formate compounds with interesting properties have been obtained through this strategy [29–32]. In fact, we has reported two novel 3D MOFs with distinct magnetic behaviors based on dimeric Ln-seamed pyrogallol[4]-arene MONCs and formate linkers derived from the hydrolysis of *N*-methylformamide very recently [24], thus we have tried to extend our study on solvothermal synthesis of metal-pyrogallol[4]arene compounds in amide-based solvents. Fortunately, we have observed the reaction of *C*-methylpyrogallol[4]arene (PgC_1) with $Ni(NO_3)_2{\cdot}6H_2O$ in DMF/MeOH solution randomly produce discrete nickel-seamed hexameric PgC_1-based MONCs, and the 3D MOFs based on the nickel-seamed MONCs and formates. Interestingly, the abovementioned isolated and MOF structure can be controlled preparations by directly adding pyridine (Py) and formic acid (HCOOH) to the reaction conditions, respectively (Scheme 1).

The reaction of PgC_1 with $Ni(NO_3)_2{\cdot}6H_2O$ in DMF/MeOH solution (1:1, v/v; DMF = *N*,*N*-dimethylformamide) at 100 °C has randomly produced isolated hexameric pyrogallol[4]arene MONC (**1**, $[Ni_{24}(PgC_1)_6(HCOO)_2(H_2O)_{44}]$), and 3D MOF (**2**, $[Ni_{24}(PgC_1)_6(HCOO)_6(MeOH)_6(H_2O)_{30}]_n$) based on the nickle-seamed MONCs as NBBs and formate ligands as linkers. Notably, controlled self-assembly of the isolated and 3D structures can be achieved by changing synthesized conditions. With the introduction of formic acid, only **2** can be obtained within the same batch. In fact, the formation of nanocapsule **1** is indeterminate and random, and we cannot make sure of the detailed experimental condition of the formation. However, we can obtain another isolated MONC (**3**, $[Ni_{24}(PgC_1)_6(Py)_{16}(H_2O)_{32}]$) *via* using the Py molecules, which coordinate at the capsule surface prevents them from assembling into hierarchical structures and leads to the formation of discrete nickel-seamed pyrogallol[4]arene nanocapsules.

Single crystal X-ray diffraction (SCXRD) analysis suggests that nanocapsule **1** crystallizes in the monoclinic space group *C2/c* and consists of a truncated octahedral Ni_{24} core housed by six PgC_1 molecules (Fig. 1a). The overall geometry of **1** is similar to the previously reported divalent V, Mn, Co, Ni, Cu or Zn seamed hexameric nanocapsules [33–37]. The 24 Ni centers can be divided into 8 nearly equilateral Ni_3 clusters, situated at the face of the truncated octahedron, which are held together by three Pg units from different PgC_1 ligands. Further analysis shows that three Ni centers are linked by three phenoxyl oxygen atoms to form a six-membered planar Ni_3O_3 array with Ni···O distances in the range from 1.985 Å to 2.038 Å, O-Ni-O angels range from 98.23°-99.64°, and Ni-O-Ni angels range from 139.74°-141.27°. In the eight Ni_3O_3 arrays, all the Ni centers are six-coordinated with an octahedral geometry, but they can be divided into two types (with half in type A, and the other half in type B) according to the specific coordinated components. For type A, the equatorial positions are occupied by nine oxygen atoms from three different PgC_1 ligands and the axial positions are occupied by six water molecules (Fig. 1b). For type B, the only difference is that one of the inner axial water molecules is replaced by the oxygen from formate ligand (Fig. 1c). The extended view of **1** along the [010] direction shows that the nanocapsules are stacked parallel with each other (Fig. 1d).

With the using of pyridine, discrete nanocapsule **3** is prepared, which has similar truncated octahedral Ni_{24} core as in **1** (Fig. 2a). The noticeable difference is that nanocapsule **3** crystallizes in the cubic space group *Fm-3c*, and its exterior surface is coordinated by 16 Py and 8 water molecules (Fig. 2b). These make **3** have much difference in the packing mode compared to **1**. Specifically, the extended view of **3** along the [010] direction shows that the nanocapsules are offset with regard to each other (Fig. 2c).

When the formic acid is introduced, MONC-based MOF **2** is obtained. SCXRD analysis reveals that **2** crystallizes in the hexagonal system with space group *R-3*, which is made up of hexameric PgC_1-based Ni_{24} NBBs and formate linkers (Fig. 3a). The overall geometry of this Ni_{24} NBB is similar to the aforementioned **1** and **3**, except that its outer axial positions are occupied by 6 methanol, 6 water molecules and 12 formate anions. Within this structure, there are two types of Ni_3O_3 arrays with six in type A and two in type B. For type A, the axial outer positions are occupied by one methanol molecules and two formate anions (Fig. 3b). For Type B, all axial outer ligands are coordinated by water molecules (Fig. 3c). An extended view from the [001] direction of **2** shows that each PgC_1-based Ni_{24} NBB is connected with six NBBs by six double formate linkers to form a 3D MOF structure (Fig. 3d). Notably, **2** is much different from the reported two hierarchical structures constructed from PgC_3OH-based Ni_{24} NBBs *via* Ni–oxygen(hydroxyl)

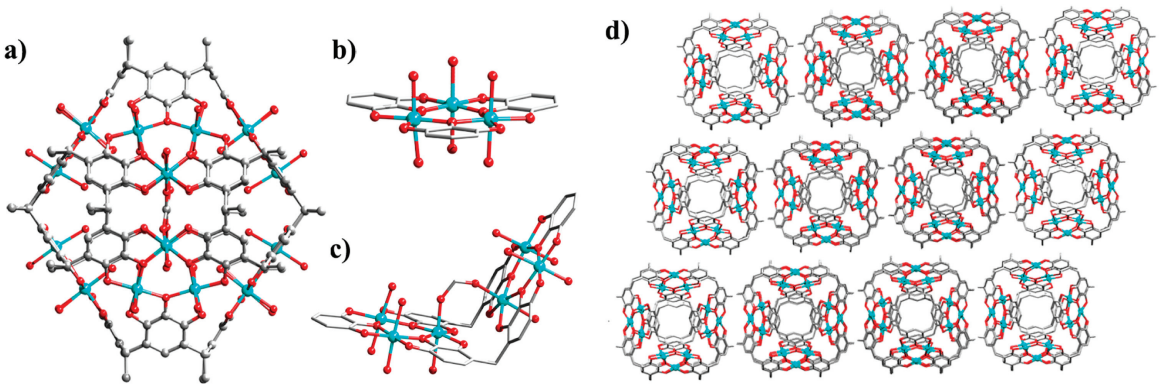

Fig. 1. (a) Molecular structure of MONC **1**. (b, c) Metal-ligand arrangement within MONC **1**. (d) Extended view of MONC **1** along [010] direction.

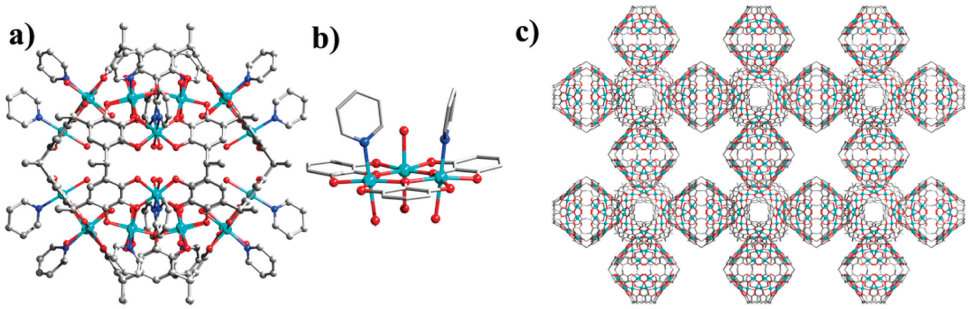

Fig. 2. (a) Molecular structure of MONC **3**. (b) Metal-ligand arrangement within MONC **3**. (c) Extended view of MONC **3** along [010] direction.

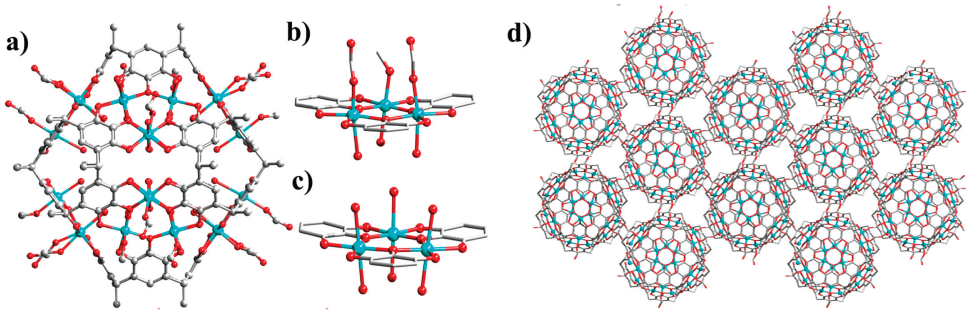

Fig. 3. (a) Molecular structure the PgC_1-based Ni_{24} NBB within **2**. (b, c) Metal-ligand arrangement within **2**. (d) Extended view of **2** along [001] direction.

coordination. Specifically, for one hierarchical structure, although each PgC_3OH-based Ni_{24} NBB is also connected with six NBBs, it forms a 2D framework structure (Fig. S1 in Supporting information) [27]; for the other one, each capsule is connected with eight adjacent nanocapsules and forms a 3D 8-connected MOF (Fig. S2 in Supporting information) [28]. To our best of knowledge, **2** presents the first example of 3D MOF structure constructed from PgC_n-based hexameric MONCs and secondary linkers.

Polynuclear transition compounds may display interesting magnetic properties including magnetization dynamics, spin frustration, spin canting and metamagnetism. Therefore, the magnetic behaviors of **2** and **3** have been studied. The variable-temperature direct current magnetic susceptibilities of **2** and **3** were recorded in the temperature range from 2.0 K to 300 K in an applied magnetic field of 1 kOe. As can be seen from Fig. 4, the χ_mT values at 300 K are 24.80 and 24.75 cm^3 K/mol for **2** and **3**, respectively, which are closed to the expected values of 24.00 cm^3 K/mol for 24 spin-only value Ni^{II} ions. As the temperatures, and reach the values of 14.89 and 14.98 cm^3 K/mol at 2.0 K. As can be seen from Figs. S3 and S4 (Supporting information), fitting the reciprocal molar magnetic susceptibilities of **2** and **3** with Curie–Weiss law ($1/\chi_m$ = T/C – θ/C) in the range of 2–300 K give C = 24.79 and 24.64 cm^3 K/mol and Weiss constants of θ = -3.49 and -3.51 K for **2** and **3**, respectively. The above features all indicate the existence of antiferromagnetic interactions among the Ni^{II} centers. Notably, **2** and **3** show much similar in magnetic properties, suggesting the six-coordinated octahedral ligand field environments mainly determine the magnetic behaviors of **2** and **3**, while the packing modes influence little in this case.

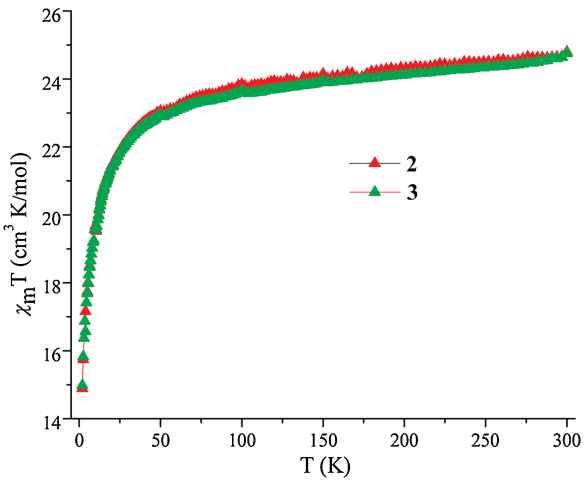

Fig. 4. Temperature dependence of magnetic susceptibilities of **2** and **3** in a 1000 Oe field.

In conclusion, we have shown the random to controlled syntheses of nickel-seamed hexameric pyrogallol[4]arene MONC-based MOF. In the present case, the *in-situ* generated formate from DMF plays an important role in the resulted structures of the products. If the formate as functional ligands at the outer MONC surface, 3D MONC-based MOF formed; while if the formate is coordinated to the inner MONC surface, discrete MONC yielded. Notably, the behavior of the formate is uncontrollable. However, directly introducing formic acid can guarantee the formation of 3D MONC-based MOF. Further work will focus on using others, especially the longer auxiliary ligands to create pyrogallol[4]arene MONC-based MOFs.

Declaration of competing interest

The authors declare that they have no known competing financial interests or personal relationships that could have appeared to influence the work reported in this paper.

Acknowledgments

This work was financially supported by the Strategic Priority Research Program of the Chinese Academy of Sciences (No. XDB20000000), the National Nature Science Foundation of China (No. 51603206) and the Nature Science Foundation of Fujian Province (No. 2016J05056).

Appendix A. Supplementary data

Supplementary material related to this article can be found, in the online version, at doi:https://doi.org/10.1016/j.cclet.2019.11.047.

References

[1] A.J. McConnell, C.S. Wood, P.P. Neelakandan, J.R. Nitschke, Chem. Rev. 115 (2015) 7729–7793.
[2] M. Hien Duy, T. Ngoc Minh, H. Yoo, Coord. Chem. Rev. 387 (2019) 180–198.
[3] C. Lu, M. Zhang, D. Tang, et al., J. Am. Chem. Soc. 140 (2018) 7674–7680.
[4] T.R. Cook, Y.-R. Zheng, P.J. Stang, Chem. Rev. 113 (2013) 734–777.
[5] W. Lu, Z. Wei, Z.Y. Gu, et al., Chem. Soc. Rev. 43 (2014) 5561–5593.
[6] J.J.I.V. Perry, J.A. Perman, M.J. Zaworotko, Chem. Soc. Rev. 38 (2009) 1400–1417.
[7] K. Li, K.H. He, Q.W. Li, et al., Chin. Chem. Lett. 30 (2019) 499–501.
[8] S.P. Wang, S.H. Hou, C. Wu, Y.J. Zhao, X.B. Ma, Chin. Chem. Lett. 30 (2019) 398–402.
[9] P. Jing, S.Y. Zhang, W. Chen, et al., Chem. Eur. J. 24 (2018) 3754–3759.
[10] S. Zhang, H. Li, E. Duan, et al., Inorg. Chem. 55 (2016) 1202–1207.
[11] X. Meng, X. Zhang, Y. Bing, et al., Inorg. Chem. 55 (2016) 12938–12943.
[12] S.I. Swamy, J. Bacsa, J.T.A. Jones, et al., J. Am. Chem. Soc. 132 (2010) 12773–12775.
[13] Z. Niu, S. Fang, X. Liu, et al., J. Am. Chem. Soc. 137 (2015) 14873–14876.
[14] L. Zhang, L. Xiang, C. Hang, et al., Angew. Chem. Int. Ed. 56 (2017) 7787–7791.
[15] Y. Kim, J. Koo, I.C. Hwang, et al., J. Am. Chem. Soc. 140 (2018) 14547–14551.
[16] C.J. Brown, F.D. Toste, R.G. Bergman, K.N. Raymond, Chem. Rev. 115 (2015) 3012–3035.
[17] Y. Fang, J.A. Powell, E. Li, et al., Chem. Soc. Rev. 48 (2019) 4707–4730.
[18] T. Hasell, A.I. Cooper, Nat. Rev. Mater. 1 (2016) 16053.
[19] C.H. Sun, X.Q. Zhao, Y.C. Li, S.P. Pang, Chin. Chem. Lett. 21 (2010) 572–575.
[20] H. Kumari, C.A. Deakyne, J.L. Atwood, Acc. Chem. Res. 47 (2014) 3080–3088.
[21] P. Jin, S.J. Dalgarno, J.L. Atwood, Coord. Chem. Rev. 254 (2010) 1760–1768.
[22] A.S. Rathnayake, H.W.L. Fraser, E.K. Brechin, et al., J. Am. Chem. Soc. 140 (2018) 15611–15615.
[23] A.S. Rathnayake, H.W.L. Fraser, E.K. Brechin, et al., J. Am. Chem. Soc. 140 (2018) 13022–13027.
[24] K.Z. Su, M.Y. Wu, W.J. Wang, et al., Sci. China Chem. 61 (2018) 664–669.
[25] D.A. Fowler, A.V. Mossine, C.M. Beavers, et al., J. Am. Chem. Soc. 133 (2011) 11069–11071.
[26] A.V. Mossine, C.M. Mayhan, D.A. Fowler, et al., Chem. Sci. 5 (2014) 2297–2303.
[27] C. Zhang, R.S. Patil, C. Liu, C.L. Barnes, J.L. Atwood, J. Am. Chem. Soc. 139 (2017) 2920–2923.
[28] C. Zhang, F. Wang, R.S. Patil, et al., Chem. Eur. J. 24 (2018) 14335–14340.
[29] D.N. Dybtsev, H. Chun, S.H. Yoon, D. Kim, K. Kim, J. Am. Chem. Soc. 126 (2004) 32–33.
[30] Y.Q. Wang, R. Cao, W.H. Bi, et al., Microporous Mesoporous Mater. 91 (2006) 215–220.
[31] X.Y. Wang, Z.M. Wang, S. Gao, Chem. Commun. (2007) 1127–1129.
[32] J.I. Choi, H. Chun, M.S. Lah, J. Am. Chem. Soc. 140 (2018) 10915–10920.
[33] K. Su, M. Wu, D. Yuan, M. Hong, Nat. Commun. 9 (2018) 4941.
[34] A.S. Rathnayake, H.W.L. Fraser, E.K. Brechin, et al., Nat. Commun. 9 (2018) 2119.
[35] H. Kumari, A.V. Mossine, S.R. Kline, et al., Angew. Chem. Int. Ed. 51 (2012) 1452–1454.
[36] A.S. Rathnayake, C.L. Barnes, J.L. Atwood, Cryst. Growth Des. 17 (2017) 4501–4503.
[37] A.S. Rathnayake, K.A. Feaster, J. White, et al., Cryst. Growth Des. 16 (2016) 3562–3564.